NEOPLASMA accepted, ahead of print manuscript
Cite article as https://doi.org/10.4149/neo_2026_251111N476

Running title: IL-17 promotes proliferation via LINC01518/miR-20a-5p/E2F1

IL-17 promotes H1299 cell proliferation via LINC01518/miR-20a-5p/E2F1 axis in non-small cell lung cancer

Chenhui Zhao[1,2,#], Yuting Ruan[3,4,#], Junjin Liao[3,4], Shuai Ying[3,4], Ningxia Wu[3,4], Pei Ma[1,2], Jing Wu[1,2], Yingwei Wang[3,4], Yongqian Shu[1,2,*], Wen Qiu[3,4,*]

[1]Department of Oncology, The First Affiliated Hospital of Nanjing Medical University, Nanjing, China; [2]Jiangsu Key Laboratory of Cancer Biomarkers, Prevention and Treatment, Collaborative Innovation Center for Cancer Personalized Medicine, Nanjing Medical University, Nanjing, China; [3]Department of Immunology, Nanjing Medical University, Nanjing, China; [4]Key Laboratory of Immunological Environment and Disease, Nanjing Medical University, Nanjing, China

*Correspondence: shuyqtg@126.com; qiuwen@njmu.edu.cn

[#]Contributed equally to this work.

Received November 11, 2025 / Accepted May 22, 2026

Human non-small cell lung cancer (NSCLC) is an inflammation-related disease. Although IL-17-induced NSCLC cell proliferation that can be regulated by transcription factors has been demonstrated, the role and mechanism of other regulatory molecules, such as long noncoding RNAs (lncRNAs), in cell proliferation remains unclear. In this study, we screened and verified the expression of aberrant lncRNAs in NSCLC cell lines (H1299 and PC9) stimulated with IL-17, and found that LINC01518 was not only overexpressed, but also enhanced cell proliferation through IL-17/IL-17RA. Further mechanism investigation discovered that IL-17-upregulated LINC01518 was mainly localized in the cytoplasm, and it could combine with miR-20a-5p through a "sponge" function, decreasing miR-20a-5p induction, while LINC01518 and miR-20a-5p co-overexpression could partially reverse the cell proliferation mediated by LINC01518 alone. LINC01518 increase or miR-20a-5p decrease could elevate E2F1 level boosting H1299 cell proliferation exposed to IL-17, while miR-20a-5p and E2F1 co-overexpression partially restored the cell proliferation inhibition from miR-20a-5p upregulation. Besides, the xenograft tumor experiments of mice confirmed that LINC01518 overexpression indeed promoted tumor growth, cell proliferation, miR-20a-5p downregulation, and E2F1 upregulation. While LINC01518 knockdown reduced tumor growth, cell proliferation, miR-20a-5p downregulation, and E2F1 upregulation induced by IL-17 stimulation. Taken together, these findings reveal that the LINC01518/miR-20a-5p/E2F1 axis contributes to IL-17-induced cell proliferation in NSCLC.

Key words: NSCLC; IL-17; proliferation; LINC01518; miR-20a-5p; E2F1

Non-small cell lung cancer (NSCLC), accounting for more than 85% of all lung cancer cases, is the most contributor to cancer mortality worldwide [1-3]. Many researches have reported that NSCLC tumorigenesis and progression are associated with the overexpression of some cytokines or

mediators, and the upregulation of these factors in NSCLC microenvironment can induce the cancer cell proliferation, migration, invasion, including other chang such as T cell or NK cell rection [4-7]. Our previous studies have disclosed that interleukin (IL)-17, as a pro-inflammatory cytokine, can enhance NSCLC cell proliferation and metastasis, and the underlying mechanism is involved in the transcriptional regulation or protein posttranslational modifications (PTMs) in IL-17-stimulated NSCLC cells [8-10]. However, the other regulative mechanism about IL-17-induced NSCLC cell proliferation has not been illuminated.

Long noncoding RNAs (lncRNAs) are classes of long-length (> 200 nucleotides) nonprotein-coding RNAs (ncRNAs) [11,12]. Numerous documents have showed that aberrantly expressed lncRNAs can modulate the proliferation of various cancer cells, including NSCLC [12-17], and some lncRNAs are recognized as cancer promoter or suppressor in cancer progression [18-20]. Furthermore, the mechanism studies have found that mostly upregulated lncRNAs can act as competing endogenous RNAs (ceRNAs) combining with some microRNAs (miRNAs) via a "sponge" function, which can reduce target gene inhibition mediated by miRNA causing the behavior alteration of cancer cells [21-23]. For instance, lncRNA LINC00665 can promote ovarian cancer (OC) cell proliferation by targeting miR-181a-5p/FHDC [12], and lncRNA PSMA3-AS1 enhances NSCLC progression through targeting miR-17-5p/PD-L1 [14], as well as lncRNA DLGAP1-AS1 can boost cell proliferation in hepatocellular carcinoma (HCC) via sequestering miR-486-5p [21]. Because up to now, little is known about whether some lncRNAs participate in the process of IL-17-triggered NSCLC cell proliferation, we thus attempt to find the abnormal lncRNAs for exploring their role and mechanism in IL-17-induced NSCLC cell proliferation.

miRNAs that belong to single-stranded short RNAs with short lengths (approximately 19-24 nucleotides) can negatively modulate target gene expression, which involves in miRNA binding to target mRNA at 3' UTR to mediate post-transcriptional gene silence or target mRNA translational repression, including degradation [24-26]. For example, LINC01518 can regulate the proliferation and migration in TGF-β1-treated human tenon capsule fibroblast cells via hsa-miR-216b-5p [22], and lncRNA SNHG17 can impact the cell proliferation and invasion by targeting miR-338-3p/SOX4 in esophageal squamous cell carcinoma (ESCC) [23]. Besides, lncRNA BBOX1-AS1 also regulates the miR-382-5p/CBX3 pathway to affect the proliferation of glioblastoma cells [27]. These mentioned-above documents suggest that the interaction of lncRNA-miRNA-mRNA plays an important role in cancer cell proliferation. Nevertheless, although lncRNA-miRNA-mRNA in the cell proliferation from different cancers has been demonstrated [27-30], whether exists the similar axis in IL-17-mediated NSCLC cell proliferation is still elusive.

To response this problem mentioned-above, in this study, we first screened differentially expressed

lncRNAs in NSCLC cells lines (H1299 and PC9) stimulated with IL-17 for 3h by high-throughput sequencing. Then, we validated markedly ten elevated lncRNAs that has been proved to possess pro-proliferative function [11, 13, 14, 17, 21, 26, 27, 31-33]. Next, we chose the upregulated LINC01518 to explore its function and regulatory mechanism in IL-17-induced NSCLC cell proliferation.

Materials and methods

Cell lines, antibodies, reagents and animals. Human BEAS-2B bronchial epithelial cell line and NSCLC cell lines such as PC9, H1299 and H1975 were purchased from American Type Culture Collection (ATCC) or European Collection of Authenticated Cell Cultures (ECACC). Anti-IL-17RA (#ab180904), anti-E2F1 (#A2067) and anti-Ki67 (#A20018) Abs were supplied by Abcam (Cambridge, UK) or ABclonal Biotech (Wuhan, China). Anti-ARHGAP12 (#PA5-51384) Ab was from Thermo Fisher Scientific (Waltham, MA, USA). Anti-TSG101 (#28283-1-AP) and anti-CDKN1A (#10355-1-AP) Abs were purchased by Proteintech (Wuhan, China). HRP-conjugated anti-rabbit IgG (#BL003A) and HRP-conjugated anti-mouse IgG (#BL001A) were from Biosharp Biotech (Hefei, China). Anti-β-actin (#AF0003), RIPA lysis buffer (#P0013B) and BCA assay kit (#P0012) were provided by Beyotime Biotech (Beijing, China). Recombinant human IL-17A (#317-ILB-050) was provided by R&D Systems (Minneapolis, MN, USA). Lipofectamine 2000 (#11668019), PARIS™ kit protein and RNA isolation system (AM1921) were from Thermo Fisher Scientific (Waltham, MA, USA). RNA isolater total RNA extraction reagent (#R401-01), HiScript II Q RT SuperMix for qPCR (#R222-01), 2× Taq Plus Master Mix (#P212-01), AceQ qPCR SYBR Green Master Mix (#Q141-02) and cell counting kit-8 (CCK-8, #A311-01) were purchased from Vazyme Biotech (Nanjing, China). Cell-Light™ EdU Apollo®567 kit (#C10310-1), crystal violet (#548-62-9), anti-LINC01518, anti-U6 (#lnc110101) and anti-18s (#lnc110102) oligodeoxynucleotide probes were provided by Sigma-Aldrich (St. Louis, MO, USA) or RiboBio (Guangzhou, China). The dual-luciferase reporter assay kit (#E1910) was from Promega (Madison, WI, USA). Male BALB/c nude mice (4-5 weeks-old) were purchased from the Animal Core facility of Nanjing Medical University.

Cell culture and IL-17 stimulation. Cells were seeded into a 60 mm dish (8×10^5 cells/dish) and incubated in Dulbecco's Modified Eagle's Medium (DMEM) with 10% fetal bovine serum (FBS) at 37 °C containing 5% CO_2. When the cell density reached 80-90%, 50 ng/ml IL-17 in according to our previous experiments [8-10] was added to the cells for the fixed time (i.e.,1 h, 2 h, 3 h, 6 h, 12 h, or 48 h, 72 h, 96 h, 8 d) after the cells were starved for 24 h.

Plasmid construction and cell transfection. The full-length of human LINC01518 (NR_120659.1)

sequence or the open reading frame (ORF) of E2F1 cDNA (NM_005225.3) were synthesized and subcloned into pcDNA3.1 vector by General Biotech (Chuzhou, China). The shRNA plasmids were constructed via cloning target sequences (Table S2) into pGPU6/GFP/Neo. SiIL-17RA and pIRES2-IL-17RA plasmids were prepared by GenePharma (Shanghai, China) and General Biotech (Chuzhou, China), respectively. Moreover, miR-20a-5p mimic or inhibitor and the matched negative controls were synthesized by RiboBio, and the sequences were: miR-20a-5p mimic forward oligos, 5'-UAAAGUGCUUAUAGUGCAGGUAG-3'; miR-20a-5p mimic reverse oligos, 5'-CUACCUGCACUAUAAGCACUUUA-3'; miR-20a-5p inhibitor oligos, 5'-CUACCUGCACUAUAAGCACUUUA-3'. All plasmids (1 μg/ml), miR-20a-5p mimic (50 nM) and miR-20a-5p inhibitor (100 nM) were transfected into cells with Lipofectamine 2000 for 48 h, and the cells transfected shRNA for 48 h were followed by 50 ng/ml IL-17 for the corresponding time.

LncRNA high-throughput sequencing. The lysates from IL-17-stimulated or -unstimulated H1299 and PC9 cells for 3 h were mixed, then sent to Bohao Biotech (Shanghai, China) for LncRNA high-throughput sequencing. The sequencing results were analyzed and partly up-regulated LncRNAs were verified.

Reverse transcription-polymerase chain reaction (RT-PCR). Cell RNA was extracted by total RNA extraction reagent. 500 μg RNA, 2 μl HiScript II Q RT SuperMix for PCR and DEPC water were mixed for converting RNA into cDNA. Thereafter, PCR assay was performed on an ABI 2720 thermal cycler with 95 °C for 5 min followed by 35 cycles of denaturation at 94 °C for 30 sec, annealing at 60 °C for 30 sec and extension at 72 °C for 30 sec, finally repetitive extension at 72 °C for 7 min. The amplification products were analyzed by agarose gel electrophoresis. GAPDH was used as an internal control, and the primer sequences are shown in Supplementary Table S1.

Real time quantitative PCR (qPCR). The qPCR was carried out using AceQ qPCR SYBR Green Master Mix on an ABI 7300 system under 95 °C/5 min, 40 cycles of 95 °C/10 sec and 60 °C/30 sec, 95 °C/15 sec, 60 °C/30 sec, 95 °C/15 sec. The results were normalized to β-actin, and the primer sequences were also listed in Table S1. Besides, miR-20a-5p expression was determined by stem-loop RT-qPCR and U6 was used as an endogenous control. The primer sequence is: miR-20a-5p, stem-loop RT, 5′-GTCGTATCCAGTGCAGGGTCCGAGGTATTCGCACTGGATACGACCTACCT-3′, forward, 5′-GCGCGTAAAGTGCTTATAGTGC-3′, reverse, 5′-AGTGCAGGGTCCGAGGTATT-3′. The qPCR results were analyzed using the $2^{-\Delta\Delta ct}$ method.

Western blot (WB). Total protein was extracted from the cells and tumor tissues using RIPA lysis buffer and measured by BCA assay kit. Then equal quantities of protein (30 μg/lane) were subjected

to 10% SDS-PAGE gel and electro-transferred onto polyvinylidene fluoride (PVDF) membrane from Millipore (Bedford, MA, USA). Subsequently, the membranes were blocked with 5% milk and incubated with the Abs against IL-17RA, or E2F1 (dilution 1:1,000) overnight followed by HRP-conjugated anti-rabbit and anti-mouse IgG (dilution 1:10,000) for 40 min. Immunolabelling was visualized by enhanced chemiluminescent (ECL) system, and band intensities were quantified by densitometry using Quantity One software (Bio-Rad, Hercules, CA, USA).

CCK-8 test. The cells were transfected with different plasmids for 48 h followed by with or without IL-17 (50 ng/ml) stimulation for the fixed time (24 h, or 48 h, 72 h, 96 h). Afterwards, the cells were incubated with 10 μl CCK-8 reagent for 1 h, and the optical density (OD) was measured at 450 nm at a wavelength of 450 nm using Synergy HTX multi-mode reader (Bio-Tek, Burlington, VT, USA). Triplicate wells were assayed for each experiment, and the actual OD values were obtained by subtracting the OD values of blank control group from the average OD values of each group.

Ethynyldeoxyuridine (EdU) assay. The cell proliferation was determined with a Cell-Light™ EdU Apollo®567 kit. Briefly, the cells were incubated with 100 μl EdU (10 μM) for 2 h plus 4% paraformaldehyde for 40 min, permeabilized in 0.5% Triton X-100 for 10 min, and stained with Apollo fluorescent dye solution for 30 min. Then, the cell nuclei were stained with 5 μg/ml Hoechst staining for 30 min. Images were observed and captured by a fluorescence microscope. The cell proliferation (at 48 h and 72 h after 50 ng/ml IL-17 treatment) was evaluated by calculating the ratios of EdU-positive cells to total cells (Hoechst-positive cells).

Colony formation assay. Cells were seeded as 300 cells/35 mm cultured dish with DMEM, and treated with the same methods as CCK8 test. Next, the cells culture medium was changed every 3 d. After the visible cell clones were observed at 8 d, the cells were fixed with methanol for 20 min plus 0.1% crystal violet staining for 20 min, and the number of cell clones upon IL-17 for 8 d was counted by naked eyes.

Cytoplasmic and Nuclear fractionation. Cytoplasmic and nuclear RNA was exacted by PARIS™ kit protein and RNA isolation system according to the manufacturer's instruction and reverse-transcribed into cDNA. The LINC01518 expression in cytoplasm and nucleus exposed to IL-17 for 3 h was determined by qPCR (β-actin as a cytoplasmic control and U6 as a nuclear control).

Fluorescence in situ hybridization (FISH). Cells were fixed in 4% formaldehyde for 2 h and permeabilized in 0.5% Triton X-100, as well as pre-hybridized for 30 min at 37 °C. Thereafter, anti-LINC01518, anti-U6 and anti-18s oligodeoxynucleotide probes were added into the hybridization solution at 37 °C overnight. Finally, the cells were counterstained with 4′, 6-diamidino-2-phenylindole (DAPI) and imaged using a confocal laser scanning microscope (Zeiss

LSM710, Germany). Besides, the percentage of signal in cytoplasm and nucleus was calculated by ImageJ.

Dual-luciferase reporter assay. The potential sequence of miR-20a-5p binding site in LINC01518 was predicted using RNAhybrid (https://bibiserv.cebitec.uni-bielefeld.de/rnahybrid). Luciferase plasmids containing the binding sequence (5′-CTCCGTTTGGCAGCCACTTTTAATAAAGCATTTTTCACTG-3′) and its mutant sequence (5′-CTCCGTTTGCGAGCGTGATTTAATATTCGTAAAATCACTG-3′) were synthesized by RiboBio, termed as LINC01518-WT and LINC01518-Mut. Then, LINC01518-WT or LINC01518-Mut plasmids along with miR-20a-5p mimic, or control mimic were respectively transfected into the cell for 48 h. The relative luciferase activity was detected by a dual-luciferase reporter assay kit in accordance to the kit' procedure, and expressed by the ratio of firefly fluorescence to renilla luciferase fluorescence.

Bioinformatics analysis. TANRIC database (https://ibl.mdanderson.org/tanric/_design/basic/main.html) was used to download LINC01518 expression in 488 NSCLC tissues and 58 paracancer tissues. InCAR database (https://lncar.renlab.org/explorer) was employed to analyze the correlation between LINC01518 expression and 131 NSCLC patient′s prognosis. LncBase (https://diana.e-ce.uth.gr/lncbasev3/home), miRanda (http://www.microrna.org/microrna/home.do) and RNA22 (https://cm.jefferson.edu/rna22/) were used to predict the miRNAs that could bind to LINC01518. StarBase (https://starbase.sysu.edu.cn/), miRDB (https://mirdb.org/), mirDIP (https://ophid.utoronto.ca/mirDIP/index.jsp) and TarBase (https://www.targetscan.org/vert_80/) were used to analyze some target genes that could bind to miR-20a-5p. GEPIA2 database (https://gepia2.cancer-pku.cn) was employed to show the expression level of E2F1, Rho GTPase-activating protein 12 (ARHGAP12), tumor susceptibility 101 (TSG101) and cyclin-dependent kinase inhibitor 1A (CDKN1A) in NSCLC and paracancer tissues. Besides, Kaplan-Meier Plotter database (https://kmplot.com/analysis/) or StarBase database was analyzed the correlation between these gene expression and NSCLC patient′s prognosis, or predicted the site of miR-20a-5p binding to E2F1.

Lentiviral (Lv) packing and cell infection. Lentivirus carrying LINC01518 gene or shLINC01518 (i.e., Lv-LINC01518, Lv-shLINC01518) and their control (i.e., Lv-empty, Lv-shCTR) were prepared by Corues Biotechnology. For LV-shRNA infection, 2×10^5 H1299 cells were incubated with above-mentioned lentivirus at the titer of 1×10^7 TU/ml for 48 h and then subjected to selection with 2 μg/ml puromycin.

Animal experiment. BALB/c nude mice were maintained under SPF conditions, and the animal

experiments in the study were approved by the Institutional Animal Care and Use Committee of Nanjing Medical University (IACUC-2507084). For xenograft model, H1299 cells (3×10^6 in 100 μl PBS) stably infected with Lv-empty, Lv-LINC01518, Lv-shCTR or Lv-shLINC01518 were incubated with or without 50 ng/ml IL-17 for 3 h and respectively injected into the left dorsal flanks of BALB/c nude mice (n=5/group). Then, the tumor size was measured every 4 days using caliper from 8 d to 28 d. After 28 days, all mice were euthanized and sacrificed. The tumor was weighted and volume was calculated using the formula: length $\times$ width^2 $\times$ 0.5. Additinally, the tumor tissures were also used to PCR, WB and immunohistochemistry (IHC) assays for examining the corresponding parameters.

IHC detection. Paraffin sections (4 μm thickness) of the tumor tissures were pepared. Briefly, the sections were repaired with sodium citrate buffer (pH 6.0) at 94 °C for 15 min, and then sealed with 1% BSA for 1 h, followed by primary anti-Ki67 Ab (1:1,000) at 4 °C overnight. Next, the sections were incubated with HRP-labeled anti-rabbit IgG at 37 °C for 30 min. After washing with PBS, the sections were immunostained by DAB reaction, and finally the photos were taken.

Statistical analysis. Data are presented as mean±SE of three independent experiments. Statistical analysis was performed using SPSS 22.0 software (IBM Corporation, Armonk, New York, USA). Graphs were plotted using GraphPad Prism 8.0 software (San Diego, CA, USA). Student's t-test was used for comparing differences between two groups. One-way ANOVA was used for comparing differences among multiple groups and the S-N-K test was exploited for pairwise comparisons. $P < 0.05$ was considered statistically significant.

Results

NSCLC cell lines express IL-17RA and IL-17 can induce NSCLC cell proliferation. We examined IL-17RA level of NSCLC cell lines i.e., H1299, PC9 and H1975, including control BEAS-2B cell lines and found that these cells were all expressed IL-17RA, more in H1299 and PC9 cells (Supplementary Figure S1A). Then, to explore the role of IL-17 treatment in NSCLC cell proliferation, we stimulated H1299 and PC9 cells with 50 ng/ml IL-17 in accordance with our previous experiments [8-10] for the fixed time. The CCK8 and EdU assays showed that the proliferation levels of H1299 or PC9 cells at 24 h after IL-17 exposure were elevated, much more at 48 h and 72 h (Supplementary Figures S1B, S1C). Besides, the two cell colony numbers from colony formation test were also increased on the 8 d after IL-17 stimulation (Supplementary Figure S1D).

IL-17RA gene knockdown can reduce IL-17-mediated NSCLC cell proliferation. To make sure that IL-17-induced NSCLC cell proliferation is related to IL-17 binding to IL-17RA, we transfected

siIL-17RA into H1299 or PC9 cells for 48 h to silence IL-17RA (Figure 1A) followed by 50 ng/ml IL-17 stimulation for 48 h, 72 h or 8 d. Thereafter, we detected the cell proliferation using the above-mentioned assays and found that IL-17RA knockdown notably decreased the proliferation levels of the two cells exposed to IL-17 (Figures 1B-1D). The data indicates that the proliferation of H1299 and PC9 cells upon IL-17 needs IL-17 binding to IL-17RA.

IL-17 stimulation increases LINC01518 expression in H1299 and PC9 cells. To explore the mechanism of H1299 and PC9 cell proliferation induced by IL-17, we performed lncRNA high-throughput sequencing to examine differentially expressed lncRNAs in the two cell lines at 3 h after 50 ng/ml IL-17 treatment. The data displayed that there were numerous differentially expressed lncRNAs, such as 459 upregulated (≥ 2-fold) and 541 downregulated (≤ 2-fold) lncRNAs (Supplementary Figure S2A). Subsequently, we selected 10 lncRNAs (i.e., LINC01518, LINC00265, PSMA3-AS1, LINC01347, DLGAP1-AS1, OIP5-AS1, SNHG17, NUTM2A-AS1, LINC01194 and BBOX1-AS1), based on the upregulated lncRNAs, which has been reported to possess pro-proliferative function in many literatures [11, 13, 14, 17, 21, 26, 27, 31-33]. Then, we measured their expression level in the two cells stimulated with IL-17 for different time. The results from RT-PCR and qPCR showed that the levels of LINC01518, LINC00265 and PSMA3-AS1 were much elevated at 2 h, peaked 3 h among the 10 lncRNAs, especially more significant and stable of LINC01518 in H1299 cells at 3 h (Supplementary Figures S2B, S2C). Thus, we chose LINC01518 to do further experiments.

IL-17RA knockdown decrease LINC01518 expression and LINC01518 can promote IL-17-induced cell proliferation. To ascertain the effects of IL-17RA gene knockdown on IL-17-upregulated LINC01518, we not only transfected siCTR or siIL-17RA into H1299 or PC9 cells for 48 h plus IL-17 incubation for 3 h (Supplementary Figure S3A), but also transfected siIL-17RA and pIRES2-IL-17RA (to resue IL-17RA knockdown caused by siIL-17RA) into the two cell lines for 48 h followed by IL-17 stimulation for 3 h (Figure 2A, 2B). The results demonstrated that silencing IL-17RA gene markedly inhibited IL-17-induced LINC01518 increase, while silencing IL-17RA followed by IL-17RA overexpression did not inhibit LINC01518 expression, particularly in H1299 cells. These data suggest that IL-17 stimulation can elevate LINC01518 expression via IL-17 binding to IL-17RA.

It has been confirmed that LINC01518 can participate in the progress of some diseases [22, 29], hence we exploited TCGA and InCAR database to analyze relative parameters. The data from TCGA showed that LINC01518 expression in 488 NSCLC tissues was significantly higher than that in 58 paracancer tissues (Figure 2C), however only InCAR database manifested that higher level of LINC01518 was closely associated with the poor prognosis of NSCLC patients (Figure 2D).

Because the lncRNA localization influences their function and cellular behavior [34], we next observed LINC01518 localization in H1299 and PC9 cells by cytoplasmic-nuclear separation and FISH experiments. The results exhibited that IL-17-upregulated LINC01518 mainly located in the cytoplasm of H1299 and PC9 cells (Figures 2E-2G).

In order to clarify the role and mechanism of LINC01518 in regulating H1299 cells proliferation induced by IL-17, we constructed and identified pcDNA3.1/LINC01518 (Supplementary Figure S3B) or short hairpin RNAs (shLINC01518-1-3) plasmids (Supplementary Figure S3E). Afterwards, we transfected pcDNA3.1 control or pcDNA3.1/LINC01518 plasmids into cells for 48 h, or transfected shCTR control or shLINC01518-1-3 into the cells for 48 h followed by IL-17 for 3 h (Supplementary Figures S3C, S3F). The results showed that pcDNA3.1/LINC01518 obviously increased LINC01518 level (Supplementary Figure S3D), while shLINC01518-1 (termed as shLINC01518) greatly inhibited LINC01518 expression in H1299 cells in response to IL-17 (Supplementary Figure S3G).

Next, we transfected the same plasmids described-previously into H1299 cells for 48 h plus IL-17 stimulation for 48 h, or 8 d to measure the cell proliferation. The assays of CCK8, EdU, or colony formation displayed that LINC01518 overexpression improved H1299 cell proliferation, while LINC01518 knockdown remarkedly declined IL-17-induced cell proliferation (Figures 2H-2J).

IL-17 stimulation or LINC01518 upregulation suppresses miR-20a-5p expression. Given that we have confirmed that IL-17-elevated LINC01518 is mostly located in the cytoplasm, the miRNAs that can bind to LINC01518 should to be searched. Therefore, we first utilized LncBase, miRanda and RNA22 databases to predict potential miRNAs and found that there were 6, 109 and 1028 miRNAs from the three databases respectively. Further Venn diagram showed that only miR-20a-5p could combine with LINC01518 (Figure 3A), and RNAhybrid database exhibited the binding mfe is - 17.1 kcal/mol (Figure 3B). These indicate that LINC01518 may be a sponge of miR-20a-5p.

Subsequently, we prepared and transfected miR-20a-5p mimic and miR-20a-5p inhibitor, including the corresponding control into H1299 cells for 48 h, and demonstrated that the overexpression of miR-20a-5p mimic or miR-20a-5p inhibitor could significantly increase or decrease miR-20a-5p expression (Figures 3C, 3D). Then, we constructed the plasmids of wild-type (WT) and the site mutant of binding miR-20a-5p (Mut) of LINC01518, namely LINC01518-WT and LINC01518-Mut (Figures 3E, 3F), and co-transfected them with miR-20a-5p mimic or miR-20a-5p inhibitor into H1299 cells for 48 h. The dual-luciferase reporter gene assay manifested that co-transfection of miR-20a-5p mimic and LINC01518-WT obviously decreased the luciferase activity of LINC01518-WT, but co-transfection of miR-20a-5p mimic and LINC01518-Mut did not have this change (Figure 3G), implicating that miR-20a-5p can directly bind to the corresponding site of LINC01518.

Besides, to ensure that LINC01518 can regulate miR-20a-5p expression as a ceRNA, we stimulated H1299 cells with 50 ng/ml IL-17 for 1 h, 2 h, 3 h, and 6 h, or transfected pcDNA3.1/LINC01518 into H1299 cells for 48 h, or transfected shLINC01518 for 48 h plus IL-17 for 3 h. The data showed that IL-17 stimulation downregualted miR-20a-5p expression at 1 h, lower at 2 h, lowest at 3 h (Figure 3H), and LINC01518 overexpression also declined miR-20a-5p, but LINC01518 knockdown significantly reversed IL-17-induced miR-20a-5p reduction (Figure 3I).

miR-20a-5p downregulation enhances cell proliferation and LINC01518 plus miR-20a-5p overexpression can reverse LINC01518-promoted cell proliferation. To reveal the role of miR-20a-5p in regulating cell proliferation, we respectively transfected miR-20a-5p mimic or miR-20a-5p inhibitor, including the corresponding control into H1299 cells for 48 h or 8 d, and observed the change of cell proliferation. The results showed that miR-20a-5p overexpression or inhibition decreased or increased H1299 cell proliferation, respectively (Figures 4A-4C), suggesting that miR-20a-5p inhibition can promote the cell proliferation. Additionally, we also co-transfected pcDNA3.1 or pcDNA3.1/LINC01518 plasmids plus NC mimic or miR-20a-5p mimic into the cells for 48 h or 8 d, and demonstrated that only LINC01518 plus miR-20a-5p overexpression could partially reverse the increase of cell proliferation elevated by LINC01518 overexpression alone (Figures 4D-4F), indicating that LINC01518 upregulation can indeed promote H1299 cell proliferation via downregulating miR-20a-5p.

miR-20a-5p binds to E2F1 and IL-17 stimulation or miR-20a-5p inhibition can raise E2F1 level. Since that miR-20a-5p can bind to LINC01518 has been ascertained, the downstream target gene of miR-20a-5p requires to be determined. To address this, we used to the databases of StarBase, miRDB, mirDIP and TarBase to predict and intersect potential target genes. Database prediction confirmed that transcription factor E2F1, Rho GTPase-activating protein 12 (ARHGAP12), tumor susceptibility 101(TSG101), and cyclin dependent kinase inhibitor 1A (CDKN1A) could combine miR-20a-5p (Figure 5A). Afterwards, we exploited the database of GEPIA or Kaplan-Meier Plotter to analyze the expression of the four genes in NSCLC tissues as well as their correlation with NSCLC patients' prognosis. The data showed that only E2F1 expression in 483 NSCLC tissues was significantly higher than that of the 347 paracancer tissues (Figure 5B), and higher E2F1 level was along with poorer prognosis in 1925 NSCLC patients (Figure 5C). Then, we transfected miR-20a-5p mimic into H1299 cells for 48 h to observe the expression of these target genes. The data displayed that only the mRNA and protein of E2F1 were greatly decreased after miR-20a-5p overexpression (Figures 5D, 5E). Additionally, the binding site of miR-20a-5p on E2F1 was exhibited by StarBase database (Figure 5F). Furthermore, we stimulated H1299 cells with 50 ng/ml IL-17 for 1 h, 2 h, 3 h, 6 h and 12 h, or transfected miR-20a-

5p mimic or miR-20a-5p inhibitor into the cells for 48 h, and proved that IL-17 stimulation increased E2F1 expression, remarkably at 2 h, and peaked at 3 h (Figure 5G). When miR-20a-5p was overexpressed or inhibited, the mRNA and protein of E2F1 were doweregulated or upregulated, respectively (Figures 5H, 5I). These findings suggest that miR-20a-5p inhibition upon IL-17 can notably elevate E2F1 level.

LINC01518 increases E2F1 expression and E2F1, which acts as a direct downstream molecule of miR-20a-5p, advances IL-17-induced cell proliferation. At the beginning of experiment, we construced and identified pcDNA3.1/E2F1 or shE2F1 plasmids (Supplementary Figures S4A-S4H). Then, we transfected pcDNA3.1/LINC01518 or pcDNA3.1/E2F1 into H1299 cells for 48 h, or transfected shLINC01518 or shE2F1 for 48 h plus IL-17 for 3 h, 48 h, 8 d to investigate E2F1 expression at 3 h and cell proliferation at 48 h or 8 d. The results showed that LINC01518 overexpression increased E2F1 level, while LINC01518 gene knockdown effectively inhibited E2F1 upregulation exposed to IL-17 (Figures 6A, 6B). Accordingly, overexpressed or silenced E2F1 increased or decreased IL-17-stimulated cell proliferation, respectively (Figures 6C-6E). Meantime, we co-transfected miR-20a-5p mimic and pcDNA3.1/E2F1 or control plasmids into H1299 cells for 48 h, and found that co-overexpression of miR-20a-5p and E2F1 could partially restore the suppression of cell proliferation mediated by miR-20a-5p mimic alone or miR-20a-5p mimic plus pcDNA3.1 control (Figures 6F-6H). The data indicate that the changes of LINC01518, miR-20a-5p or E2F1 level can impact IL-17-induced cell proliferation by indirect or direct manner.

Next, to further determine the upstream or downstream relationship between E2F1 and LINC01518 or miR-20a-5p, we respectively transfected pcDNA3.1, pcDNA3.1/E2F1 into H1299 cells for 48 h, or transfected shCTR or shE2F1 into the cells for 48 h followed by IL-17 for 3 h. The results exhibited that after E2F1 overexpression, the level of LINC01518 and miR-20a-5p did not obviously alter, but in the cells with shCTR+IL-17 or shE2F1 + IL-17 treatment, the level of LINC01518 was increased. Additionally, the level of miR-20a-5p was still decreased, while level of LINC01518 and miR-20a-5p between the two groups (namely shCTR+IL-17 and shE2F+IL-17) had no significant difference (Figure 6I). These data confirm that E2F1 is a downstream molecule of LINC01518 and miR-20a-5p in IL-17-stimulated H1299 cells.

LINC01518 can promote tumor growth, cell proliferation and E2F1 expression of in mouse xenograft model. To evaluate the potential roles of LINC01518 in vivo, we subcutaneously injected H1299 cells that had been stably infected with Lv-empty, Lv-LINC01518, Lv-shCTR, Lv-shLINC01518 followed by IL-17 incubation into BALB/c nude mice to establish xenograft model. The groups were as follows: Lv-empty, Lv-LINC01518, Lv-shCTR+IL-17 and Lv-shLINC01518+IL-17 groups. After 28 d, the volume and weight of the tumors from Lv-LINC01518

or Lv-shLINC01518+IL-17 group were correspondingly much larger or smaller compared to Lv-empty or Lv-shCTR+IL-17 group (Figures 7A-7C). Moreover, the markedly higher or lower Ki67 cells in the tumor tissue sections by IHC were seen in Lv-LINC01518 or Lv-shLINC01518+IL-17 group compared to Lv-empty or Lv-shCTR+IL-17 group (Figure 7D). Meanwhile, the upregulating LINC01518, E2F1 and reducing miR-20a-5p, as well as decreasing LINC01518, E2F1 and increasing miR-20a-5p of the tumor tissues in Lv-LINC01518 or Lv-shLINC01518+IL-17 was also confirmed by qPCR and WB assays (Figures 7E-7G).

Discussion

LncRNAs have been widely identified and researched in diverse types of cancers, including NSCLC [11-20]. Our former studies have confirmed that the progression of NSCLC partly contributes to IL-17 overexpression, and the increased IL-17 in the cancer tissues can promote the proliferation and invasion of NSCLC cells [8-10]. In the present study, we first screened and validated the change of lncRNA expression in NSCLC cells (H1299 and PC9) stimulated with IL-17 and found that many lncRNAs were markedly upregulated. Among these elevated lncRNAs, LINC01518 exhibited higher level via IL-17 binding to IL-17RA on H1299 and PC9 cells. Meantime, we further overexpressed or silenced LINC01518 gene in the two cells and proved that LINC01518 upregulation or downregulation could correspondingly increase or decrease the proliferation of H1299 and PC9 cells. These findings suggest that LINC01518 upregulation upon IL-17 promotes NSCLC cell proliferation.

Previous documents have showed that LINC01518 has different roles in human diseases and cancers [22, 29]. For example, Kong N and his colleagues [22] have reported that LINC01518 can regulate the proliferation and migration in TGF-β1-treated human tenon capsule fibroblast cells through affecting hsa-miRNA-216b-5p, and Zhang D et al [29] have proposed that LINC01518 knockdown can weaken the tumorigenicity by suppression PIK3KCA/Akt pathway in OSCC. However, up to date, the role and mechanism of LINC01518 in IL-17-induced NSCLC cell proliferation remain largely unrecognized.

Several researches have noted that the function of lncRNAs is associated with its localization in cellular nucleus or cytoplasm [11, 34]. The lncRNAs in cytoplasm can act as sponge for certain miRNAs to impact cell behaviors, such as proliferation and migration [27-31]. Based on these reports, in this study, we examined LINC01518 localization and demonstrated that IL-17-upregulated LINC01518 was mostly located in the cytoplasm of H1299 and PC9 cells. Considering that many lncRNAs can negatively modulate some miRNAs, we thus used several databases to predict the miRNA that could combine with LINC01518. Thereafter, further experiments exhibited

that miR-20a-5p could directly interact with LINC01518, and its expression could be retrained by LINC01518 upregulation, indicating that LINC01518 can be as a sponge depressing miR-20a-5p induction in NSCLC cells exposed to IL-17.

In the progression of human diseases, miR-20a-5p expression can be decreased by competitively binding to lncRNA to influence the cellular functions [30, 31, 35, 36]. For instance, lncRNA FALEC can augment the cell proliferation, migration and drug resistance of cholangiocarcinoma through miR-20a-5p/SHOC2 axis [30], and lncRNA GALML3-AS1 suppresses papillary thyroid cancer via sponging miR-20a-5p/RBM38 [35]. Additionally, lncRNA HAGLR can also accelerate gastric cancer progression by affecting miR-20a-5p/E2F1 [36]. In our experiment, we found that miR-20a-5p expression was remarkably downregulated in H1299 cells stimulated by IL-17, and LINC01518 overexpression inhibited miR-20a-5p, and LINC01518 knockdown restored miR-20a-5p expression. Further investigation exhibited that LINC01518 could competitively combine with the corresponding sequence of miR-20a-5p suppressing miR-20a-5p production, which aggravated IL-17-triggered cell proliferation, while LINC01518 and miR-20a-5p co-overexpression, the H1299 cell proliferation was markedly lower compared with LINC01518 overexpression alone. These data implicate that LINC01518 can really enhance NSCLC cell proliferation via sponging miR-20a-5p.

As we have known, the regulatory axis of lncRNA-miRNA-mRNA contributes partly to the tumorigenesis and progression of various cancers [37-39]. Meng et al. [38] have demonstrated that LINC00461 can boost the expression of transcription factor E2F1 through sponging miR-4478, and LINC00461/miR-4478/E2F1 feedback loop can advance NSCLC cell proliferation and migration. In addition, Gobbi et al. [39] have reported that lncRNA TAZ-AS202 also promotes NSCLC progression via increasing E2F1, and Huang et al. [40] have confirmed that E2F1 can cause cancer malignant behaviors by regulating cell cycle, which is related to the crosstalk between lncRNA and E2F1. Thereby, in the study, we used several databases to predict the target gene of miR-20a-5p and performed next tests, and further results uncovered that IL-17 stimulation or miR-20a-5p inhibition in H1299 cells could significantly upregulate E2F1 level, and LINC01518 overexpression was accompanied with E2F1 increase. Meanwhile, E2F1 gene overexpression or knockdown obviously raised or reduced IL-17-induced H1299 cell proliferation, but E2F1 expression increase or decrease did not affect LINC01518 and miR-20a-5p induction mediated by IL-17. Notably, E2F1 overexpression could partially restore H1299 cell proliferation, which was inhibited by miR-20a-5p, indicating that E2F1 is a downstream factor of LINC01518 and miR-20a-5p in IL-17-stimulated H1299 cells. Additionally, the in vivo experiments of mouse xenograft tumor also proved that LINC01518 upregulation could promote tumor growth, cell proliferation, miR-20a-5p inhibition, and E2F1 expression.

To summarize, the study showed that IL-17 exposure to NSCLC cells could not only upregulate LINC01518 or E2F1 and downregulate miR-20a-5p expression, but also promote the cell proliferation via binding to IL-17RA. Mechanistically, IL-17-upregulated LINC01518 was mainly localized in the cytoplasm, and as a molecular sponge, LINC01518 could inhibit miR-20a-5p production and elevate E2F1 level via combining with miR-20a-5p, leading to incresing H1299 cell proliferation upon IL-17 (Figure 7H). Overall, these findings from the experiments in vitro and in vivo discover that IL-17-triggered NSCLC cell proliferation needs the formation of LINC01518/miR-20a-5p/E2F1 axis, which offers a new insight to the pathogenesis of NSCLC cell proliferation induced by IL-17 and several potential targets for NSCLC therapy.

Acknowledgements: This work was supported by the National Natural Science Foundation of China (No. 81902878). The study was also supported by the Excellent Young or Middle-aged Teachers Project of Nanjing Medical University. We thank all the participants for this work.

Supplementary information is available in the online version of the paper.

References

[1] XU J, TIAN L, QI W, LV Q, WANG T. Advancements in NSCLC: From Pathophysiological Insights to Targeted Treatments. Am J Clin Oncol 2024; 47: 291-303. https://doi.org/10.1097/coc.0000000000001088

[2] SUNG H, FERLAY J, SIEGEL RL, LAVERSANNE M, SOERJOMATARAM I et al. Global Cancer Statistics 2020: GLOBOCAN Estimates of Incidence and Mortality Worldwide for 36 Cancers in 185 Countries. CA Cancer J Clin 2021; 71: 209-249. https://doi.org/10.3322/caac.21660

[3] BADE BC, DELA CRUZ CS. Lung Cancer 2020: Epidemiology, Etiology, and Prevention. Clin Chest Med 2020; 41: 1-24. https://doi.org/10.1016/j.ccm.2019.10.001

[4] GRETEN F R, GRIVENNIKOV SI. Inflammation and Cancer: Triggers, Mechanisms, and Consequences. Immunity 2019; 51: 27-41. https://doi.org/10.1016/j.immuni.2019.06.025

[5] LIU Y, GAO Y, LIN T. Expression of interleukin-1 (IL-1), IL-6, and tumor necrosis factor-α (TNF-α) in non-small cell lung cancer and its relationship with the occurrence and prognosis of cancer pain. Ann Palliat Med 2021; 10: 12759-12766. https://doi.org/10.21037/apm-21-3471

[6] ZHAO C, LI Y, QIU W, HE F, ZHANG W et al. C5a induces A549 cell proliferation of non-small cell lung cancer via GDF15 gene activation mediated by GCN5-dependent KLF5 acetylation. Oncogene 2018; 37: 4821-4837. https://doi.org/10.1038/s41388-018-0298-9

[7] GUO J, PENG L, MA P, MAI Y, GAO T et al. IL-15 functionalized biomimetic hybrid mRNA vaccine for enhanced NSCLC immunotherapy via synergistic activation of T cells and NK cells. Mater Today Bio 2025; 32: 101914. https://doi.org/10.1016/j.mtbio.2025.101914

[8] ZHAO C, LI Y, ZHANG W, ZHAO D, MA L et al. IL- 17 induces NSCLC A549 cell proliferation via the upregulation of HMGA1, resulting in an increased cyclin D1 expression. Int J Oncol 2018; 52: 1579-1592. https://doi.org/10.3892/ijo.2018.4307

[9] GE W, GONG Y, LI Y, WU N, RUAN Y et al. IL-17 induces non-small cell lung cancer metastasis via GCN5-dependent SOX4 acetylation enhancing MMP9 gene transcription and expression. Mol Carcinog 2023; 62: 1399-1416. https://doi.org/10.1002/mc.23585

[10] GE W, LI Y A, RUAN Y, WU N, MA P et al. IL-17 induces NSCLC cell migration and invasion by elevating MMP19 gene transcription and expression through the interaction of p300-dependent STAT3-K631 acetylation and its Y705-phosphorylation. Oncol Res 2024; 32: 625-641. https://doi.org/10.32604/or.2023.031053

[11] GHAFOURI-FARD S, SHOOREI H, BRANICKI W, TAHERI M. Non-coding RNA profile in lung cancer. Exp Mol Pathol 2020; 114: 104411. https://doi.org/10.1016/j.yexmp.2020.104411

[12] WANG S, WANG Y, LU J, WANG J. LncRNA LINC00665 Promotes Ovarian Cancer Cell Proliferation and Inhibits Apoptosis via Targeting miR-181a-5p/FHDC. Appl Biochem Biotechnol 2022; 194: 3819-3832. https://doi.org/10.1007/s12010-022-03943-3

[13] MENG F, ZHOU Y, DONG B, DONG A, ZHANG J. Long non-coding RNA LINC01194 promotes the proliferation, migration and invasion of lung adenocarcinoma cells by targeting miR-641/SETD7 axis. Cancer Cell Int 2020; 20: 588. https://doi.org/10.1186/s12935-020-01680-3

[14] CHENG G, LI Y, LIU Z, SONG X. lncRNA PSMA3-AS1 promotes the progression of non-small cell lung cancer through targeting miR-17-5p/PD-L1. Adv Clin Exp Med 2021; 30: 1043-1050. https://doi.org/10.17219/acem/138624

[15] WANG W, WEI C, LI P, WANG L, LI W et al. Integrative analysis of mRNA and lncRNA profiles identified pathogenetic lncRNAs in esophageal squamous cell carcinoma. Gene 2018; 661: 169-175. https://doi.org/10.1016/j.gene.2018.03.066

[16] HUA Q, JIN M, MI B, XU F, LI T et al. LINC01123, a c-Myc-activated long non-coding RNA, promotes proliferation and aerobic glycolysis of non-small cell lung cancer through miR-199a-5p/c-Myc axis. J Hematol Oncol 2019; 12: 91. https://doi.org/10.1186/s13045-019-0773-y

[17] KOTAKE Y, MATSUNAGA N, WAKASAKI T, OKADA R. OIP5-AS1 Promotes Proliferation of Non-small-cell Lung Cancer and Head and Neck Squamous Cell Carcinoma Cells. Cancer Genomics Proteomics 2021; 18: 543-548. https://doi.org/10.21873/cgp.20279

[18] 0YUAN K, LAN J, XU L, FENG X, LIAO H et al. Long noncoding RNA TLNC1 promotes the growth and metastasis of liver cancer via inhibition of p53 signaling. Mol Cancer 2022; 21: 105. https://doi.org/10.1186/s12943-022-01578-w

[19] ZHA LF, ZHANG LD, PAN HM, MA HD. Upregulation of lncRNA NCK1-AS1 predicts poor prognosis and contributes to non-small cell lung cancer proliferation by regulating CDK1. Eur Rev Med Pharmacol Sci 2021; 25: 1351-1357. https://doi.org/10.26355/eurrev_202102_24843

[20] FANG D, OU X, SUN K, ZHOU X, LI Y et al. m6A modification-mediated lncRNA TP53TG1 inhibits gastric cancer progression by regulating CIP2A stability. Cancer Sci 2022; 113: 4135-4150. https://doi.org/10.1111/cas.15581

[21] PENG X, WEI F, HU X. Long noncoding RNA DLGAP1-AS1 promotes cell proliferation in hepatocellular carcinoma via sequestering miR-486-5p. J Cell Biochem 2020; 121: 1953-1962. https://doi.org/10.1002/jcb.29430

[22] KONG N, BAO Y, ZHAO H, KANG X, TAI X et al. Long Noncoding RNA LINC01518 Modulates Proliferation and Migration in TGF-β1-Treated Human Tenon Capsule Fibroblast Cells Through the Regulation of hsa-miR-216b-5p. Neuromolecular Med 2022; 24: 88-96. https://doi.org/10.1007/s12017-021-08662-2

[23] CHEN W, WANG L, LI X, ZHAO C, SHI L et al. LncRNA SNHG17 regulates cell proliferation and invasion by targeting miR-338-3p/SOX4 axis in esophageal squamous cell carcinoma. Cell Death Dis 2021; 12: 806. https://doi.org/10.1038/s41419-021-04093-w

[24] BUDAKOTI M, PANWAR AS, MOLPA D, SINGH RK, BÜSSELBERG D et al. Micro-RNA: The darkhorse of cancer. Cell Signal 2021; 83: 109995. https://doi.org/10.1016/j.cellsig.2021.109995

[25] HUANG W, WU X, XIANG S, QIAO M, CEN X et al. Regulatory mechanism of miR-20a-5p expression in Cancer. Cell Death Discov 2022; 8: 262. https://doi.org/10.1038/s41420-022-01005-5

[26] WANG J, YU Z, WANG J, SHEN Y, QIU J et al. LncRNA NUTM2A-AS1 positively modulates TET1 and HIF-1A to enhance gastric cancer tumorigenesis and drug resistance by sponging miR-376a. Cancer Med 2020; 9: 9499-9510. https://doi.org/10.1002/cam4.3544

[27] TAN B, CHEN T, SONG P, LIN F, HE S et al. lncRNA BBOX1-AS1 regulates the miR-382-5p/CBX3 Signalling pathway to affect the proliferation and apoptosis of glioblastoma cells. Int Immunopharmacol 2025; 157: 114790. https://doi.org/10.1016/j.intimp.2025.114790

[28] PAN T, WANG H, WANG S, LIU F. Long Non-Coding RNA LINC01929 Facilitates Cell Proliferation and Metastasis as a Competing Endogenous RNA Against MicroRNA miR-1179 in Non-Small Cell Lung Carcinoma. Br J Biomed Sci 2022; 79: 10598. https://doi.org/10.3389/bjbs.2022.10598

[29] ZHANG D, ZHANG H, WANG X, HU B, ZHANG F et al. LINC01518 knockdown inhibits tumorigenicity by suppression of PIK3CA/Akt pathway in oesophageal squamous cell carcinoma. Artif Cells Nanomed Biotechnol 2019; 47: 4284-4292. https://doi.org/10.1080/21691401.2019.1699815

[30] DU H, HOU S, ZHANG L, LIU C, YU T et al. LncRNA FALEC increases the proliferation, migration and drug resistance of cholangiocarcinoma through competitive regulation of miR-20a-5p/SHOC2 axis. Aging (Albany NY) 2023; 15: 3759-3770. https://doi.org/10.18632/aging.204709

[31] LI X, GUO C, CHEN Y, YU F. Long non-coding RNA SNHG16 regulates E2F1 expression by sponging miR-20a-5p and aggravating proliferative diabetic retinopathy. Can J Physiol Pharmacol 2021; 99: 1207-1216. https://doi.org/10.1139/cjpp-2020-0693

[32] YU S, CUI Z, ZHOU J, WANG K, LI Q et al. LINC00265 maintains hepatocyte proliferation during liver regeneration by targeting miRNA-28-5p. Biosci Biotechnol Biochem 2021; 85: 528-536. https://doi.org/10.1093/bbb/zbaa049

[33] ZHENG G, LIU Y, YAN Z, XIE X, Xiang Z et al. Elevated LOXL2 expression by LINC01347/miR-328-5p axis contributes to 5-FU chemotherapy resistance of colorectal cancer. Am J Cancer Res 2021; 11: 1572-1585.

[34] BRIDGES MC, DAULAGALA AC, KOURTIDIS A. LNCcation: lncRNA localization and function. J Cell Biol 2021; 220. https://doi.org/10.1083/jcb.202009045

[35] ZHANG X, ZHANG X, JIA Q, LI H, MA R et al. LncRNA CALML3-AS1 suppresses papillary thyroid cancer progression via sponging miR-20a-5p/RBM38 axis. BMC Cancer 2022; 22: 344. https://doi.org/10.1186/s12885-022-09360-3

[36] LIU Q, LI Y, TAN B, ZHAO Q, FAN L et al. LncRNA HAGLR regulates gastric cancer progression by regulating the miR-20a-5p/E2F1 axis. Aging (Albany NY) 2024; 16: 11843-11856. https://doi.org/10.18632/aging.206039

[37] SHETTY A, VENKATESH T, KABBEKODU SP, TSUTSUMI R, SURESH PS. LncRNA-miRNA-mRNA regulatory axes in endometrial cancer: a comprehensive overview. Arch Gynecol Obstet 2022; 306: 1431-1447. https://doi.org/10.1007/s00404-022-06423-5

[38] MENG Q, LIU M, CHENG R. LINC00461/miR-4478/E2F1 feedback loop promotes non-small cell lung cancer cell proliferation and migration. Biosci Rep 2020; 40. https://doi.org/10.1042/bsr20191345

[39] GOBBI G, GRIECO A, TORRICELLI F, SAUTA E, SANTANDREA G et al. The long non-coding RNA TAZ-AS202 promotes lung cancer progression via regulation of the E2F1 transcription factor and activation of Ephrin signaling. Cell Death Dis 2023; 14: 752. https://doi.org/10.1038/s41419-023-06277-y

[40] HUANG P, WEN F, LI Q. Current concepts of the crosstalk between lncRNA and E2F1: shedding light on the cancer therapy. Front Pharmacol 2024; 15: 1432490. https://doi.org/10.3389/fphar.2024.1432490

Figure Legends

Figure 1. The change of IL-17-induced H1299 and PC9 cell proliferation after IL-17RA silence. A) IL-17RA expression in the cells transfected with siIL-17RA or siCTR for 48 h was detected by WB. B, C) The levels of cell proliferation transfected with siIL-17RA plus IL-17 stimulation for 48 h and 72 h were measured by CCK8 (B) or EdU (C) assay (Magnification: ×200). D) The cell colony numbers in the cells transfected with siIL-17RA plus IL-17 treatment for 8 d were examined by colony formation assay. Data were displayed as means±SE (n=3), $^{**}p < 0.01$ vs. siCTR; $^{▲▲}p < 0.01$ vs. siCTR+IL-17.

Figure 2. LINC01518 expression after silencing IL-17RA, TANRIC or InCAR database analysis, and LINC01518 licolization, as well as LINC01518 role in cell proliferation. A) The expression of IL-17RA in H1299 (up) and PC9 (down) cells transfected with pIRES2-EGFP or pIRES2-IL-17RA was determined by WB. B) The RNA of LINC01518 in H1299 and PC9 cells transfected with siCTR, siIL-17RA, pIRES2-EGFP or pIRES2-IL-17RA for 48 h plus IL-17 for 3 h was detected by qPCR, $^{**}p < 0.01$ vs. siCTR+pIRES2-EGFP; $^{▲}p < 0.05$, $^{▲▲}p < 0.01$ vs. siCTR+pIRES2-EGFP+IL-17. C) The level of LINC01518 expression was analyzed by TANRIC database, $^{*}p < 0.05$ vs. normal control. D) The correlation between LINC01518 expression and NSCLC patient's prognosis was analyzed by InCAR database. E) The cytoplasmic and nuclear levels of LINC01518 after IL-17 stimulation for 3 h were examined by qPCR (β-actin as cytoplasmic and U6 as nuclear control). F) LINC01518 localization in H1299 and PC9 cells was determined by FISH (18S as cytoplasmic and U6 as nuclear control). Magnification × 400. G) The percentage levels of

LINC01518 in cytoplasm and nucleus in H1299 and PC9 cells from FISH experiments (F). H-J) The proliferation of H1299 cells respectively transfected with pcDNA3.1, pcDNA3.1/LINC01518 for 48 h, or shCTR, shLINC01518 for 48 h followed by IL-17 48 h or 8 d were detected by CCK8 (H), EdU (I, Magnification ×200) or colony formation (J) assays. Data were presented as means±SE (n=3), **$p < 0.01$ vs. pcDNA3.1, $^{▲▲}p < 0.01$ vs. shCTR, $^{\#\#}p < 0.01$ vs. shCTR+IL-17

Figure 3. Idenfication of LINC01518 binding to miRNA, and effects of IL-17 stimulation and LINC01518 overexpression or knockdown on miR-20a-5p inducton. A) The potential miRNAs that can bind to LINC01518 were predicted by LncBase, miRanda and RNA22 databases. B) Sketch map of LINC01518 combined with miR-20a-5p site that was predicted by RNAhybrid database. C, D) MiR-20a-5p level in H1299 cells transfected miR-20a-5p mimic (C) or miR-20a-5p inhibitor (D) for 48 h was detected by qPCR, **$p < 0.01$ vs. NC mimic or NC inhibitor. E) Schematic diagram of the predicted binding between LINC01518 and miR-20a-5p. F) Partial sequencing results of LINC01518-WT and LINC01518-Mut. G) The luciferase activity was evaluated by dual-luciferase reporter assay after H1299 cells co-transfected with LINC01518-WT or LINC01518-Mut along with NC mimic or miR-20a-5p mimic for 48 h, **$p < 0.01$ vs. NC mimic. H, I) The expression of miR-20a-5p was examined by qPCR after H1299 cells stimulated with IL-17 (50 ng/ml) for 1 h, 2 h, 3 h, 6 h. (H), or transfected with pcDNA3.1 or pcDNA3.1/LINC01518 for 48 h, or shCTR and shLINC01518 for 48 h plus IL-17 for 3 h (I). All data were shown as means±SE (n=3), **$p < 0.01$ vs. 0 h or pcDNA3.1, $^{▲▲}p < 0.01$ vs. shCTR, $^{\#\#}p < 0.01$ vs. shCTR+IL-17

Figure 4. Effects of miR-20a-5p expression or inhibition and LINC01518 plus miR-20a-5p co-expression on H1299 cell proliferation. A-C) H1299 cells were respectively transfected with NC mimic, miR-20a-5p mimic, NC inhibitor and miR-20a-5p inhibitor for 48 h or 8 d, the cell proliferation level and colony number were checked by CCK8 (A), EdU (B, Magnification × 200) and colony formation (C) assays, **$p < 0.01$ vs. NC mimic, $^{▲}p < 0.05$, $^{▲▲}p < 0.01$ vs. NC inhibitor. D-F) H1299 cells were transfected with pcDNA3.1, pcDNA3.1/LINC01518, or co-transfected with pcDNA3.1/LINC01518 plus NC mimic, or miR-20a-5p mimic for 48 h or 8 d, the cell proliferation and colony number were measured by CCK8 (D), EdU (E, Magnification ×200) and colony formation (F) tests. Data were presented as means±SE (n=3), **$p < 0.01$ vs. pcDNA3.1, $^{▲▲}p < 0.01$ vs. pcDNA3.1/LINC01518+NC mimic

Figure 5. Prediction and identification of target gene that can bind to miR-20a-5p, and the change of IL-17-induced E2F1 as well as effects of miR-20a-5p expression on E2F1 production. A) The

predicted potential target genes that can bind to miR-20a-5p and their intersection by StarBase, miRDB, mirDIP and TarBase databases were showed by Venn diagram. B) The expression levels of E2F1, ARHGAP12, TSG101, CDKN1A in 483 NSCLC tissues and 347 paracancer tissues were analyzed by GEPIA database. C) The correlation between the expression of E2F1, ARHGAP12, TSG101 or CDKN1A and overall survival of 1925 NSCLC patients were analyzed by Kaplan-Meier Plotter database. D, E) The mRNA (D) and protein (E) levels of E2F1, ARHGAP12, TSG101 and CDKN1A in H1299 cells transfected with NC mimic or miR-20a-5p mimic for 48 h were detected by qPCR or WB. **$p < 0.01$ vs. NC mimic. F) The binding site of miR-20a-5p to E2F1 was showed by StarBase database. G) The expression of E2F1 in H1299 cells treated with IL-17 (50 ng/ml) for 1 h, 2 h, 3 h, 6 h and 12 h was examined by WB, *$p < 0.05$, **$p < 0.01$ vs. 0 h. H, I) The mRNA (H) and protein (I) of E2F1 were measured by qPCR and WB in H1299 cells transfected with NC mimic, miR-20a-5p mimic, or NC inhibitor, miR-20a-5p inhibitor for 48 h. Data were shown as means±SE (n = 3), **$p < 0.01$ vs. NC mimic, $^{▲▲}p < 0.01$ vs. NC inhibitor

Figure 6. Effects of expressed and silenced LINC01518 or E2F1 gene on E2F1 induction or cell proliferation and LINC01518 or miR-20a-5p expression. A, B) H1299 cells were transfected with pcDNA3.1, pcDNA3.1/LINC01518 for 48 h or shCTR, shLINC01518 for 48 h plus IL-17 for 3 h, the E2F1 mRNA (A) and protein (B) were examined by qPCR and WB, **$p < 0.01$ vs. pcDNA3.1, $^{▲▲}p < 0.01$ vs. shCTR, $^{\#\#}p < 0.01$ vs. shCTR+IL-17. C-E) H1299 cells were transfected with pcDNA3.1, pcDNA3.1/E2F1 for 48 h or shCTR, shE2F1 for 48 h followed by IL-17 for 48 h or 8 d, the cell proliferation and colony number were estimated by CCK8 (C), EdU (D) and colony formation (E) assays, **$p < 0.01$ vs. pcDNA3.1, $^{▲▲}p < 0.01$ vs. shCTR, $^{\#\#}p < 0.01$ vs. shCTR+IL-17. F-H) H1299 cells were transfected with NC mimic, miR-20a-5p mimic, or co-transfected with miR-20a-5p mimic, pcDNA3.1 or pcDNA3.1/E2F1 for 48 h or 8 d, the cell proliferation and colony number were observed by the same tests, **$p < 0.01$ vs. NC mimic, $^{▲▲}p < 0.01$ vs. miR-20a-5p mimic+pcDNA3.1. I) H1299 cells were transfected with pcDNA3.1, pcDNA3.1/E2F1 for 48 h or shCTR, shE2F1 for 48 h plus IL-17 for 3 h, the RNA of LINC01518 and miR-20a-5p was measured by qPCR, **$p < 0.01$ vs. pcDNA3.1, $^{▲▲}p < 0.01$ vs. shCTR. The photograph from EdU (Magnification ×200) and colony formation assay was showed, and data exhibited as means±SE (n=3).

Figure 7. LINC01518 can enhance mouse xenograft tumor growth, cell proliferation and relative parameter change. A) Photographs of excised tumors from BALB/c node mice (5/group) were showed in Lv-empty, Lv-LINC01518, Lv-shCTR+IL-17 groups, Lv-shLINC01518+IL-17. B, C)

Average tumor volume and weight of tumors in each group. D) Number of Ki67 cells in tumor tissue sections in each group was displayed by IHC (scale bars=100 μm). E, F) The RNA level of LINC01518 and miR-20a-5p in tumor tissues was measured by qPCR. G) The protenin expression of E2F1 in tumor tissues was detected by WB. *$p < 0.05$, **$p < 0.01$ vs. Lv-empty, ▲$p < 0.05$, ▲▲$p < 0.01$ vs. shCTR+IL-17, and the data presented as means±SE (n=5). H) A putative scheme of the mechanism about IL-17-induced NSCLC cell proliferation. LINC01518 in H1299 cytoplasm is upregulated by IL-17 binding to IL-17RA. In the process, elevated LINC01518 as a ceRNA can inhibit miR-20a-5p expression by sponging it, enhancing cell proliferation via downregulated miR-20a-5p and secondary increased E2F1. These findings reveal that LINC01518/miR-20a-5p/E2F1 axis contributes to IL-17-induced H1299 cell proliferation.

Fig. 1 [Download full resolution image]

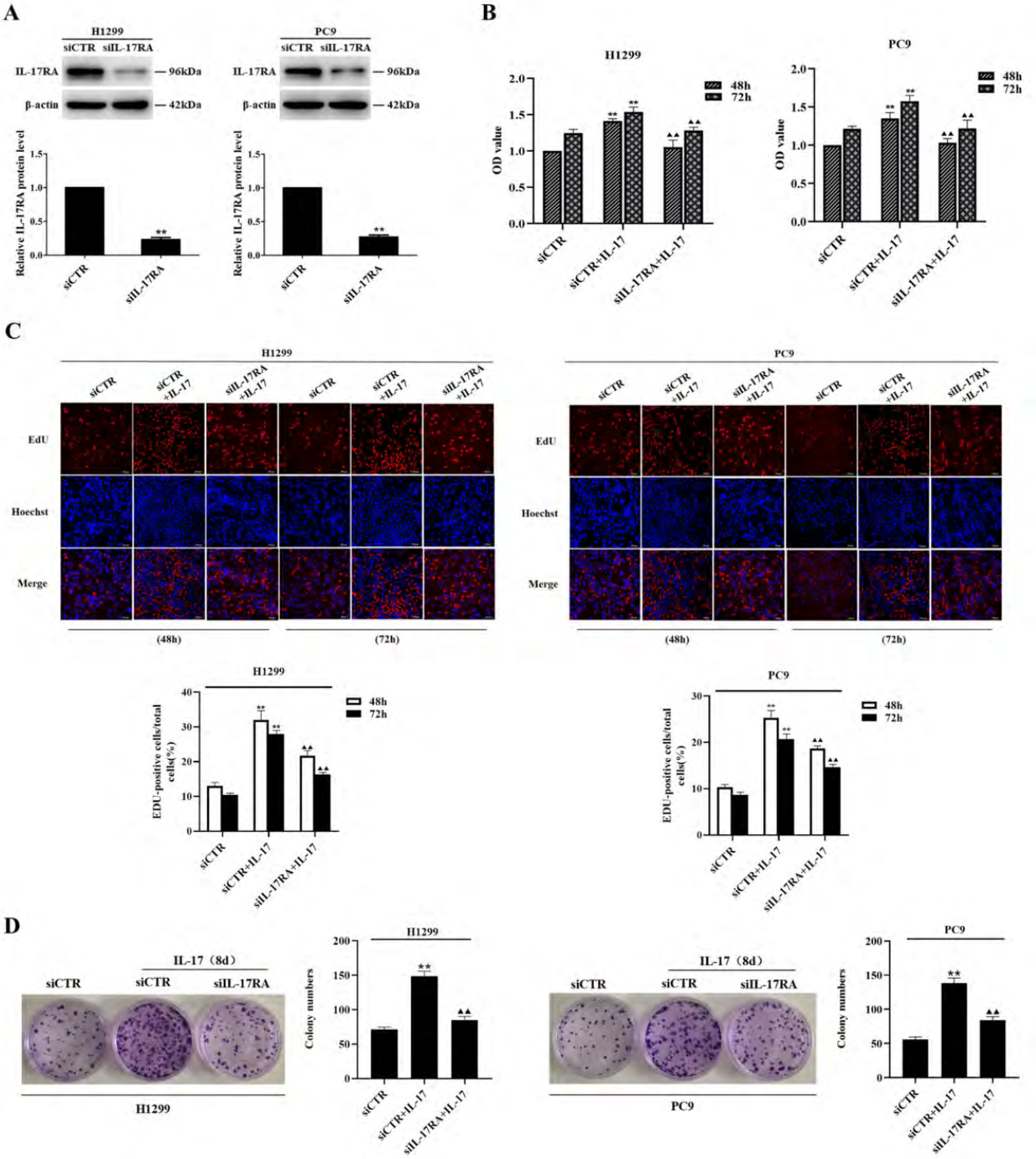

Fig. 2 [Download full resolution image]

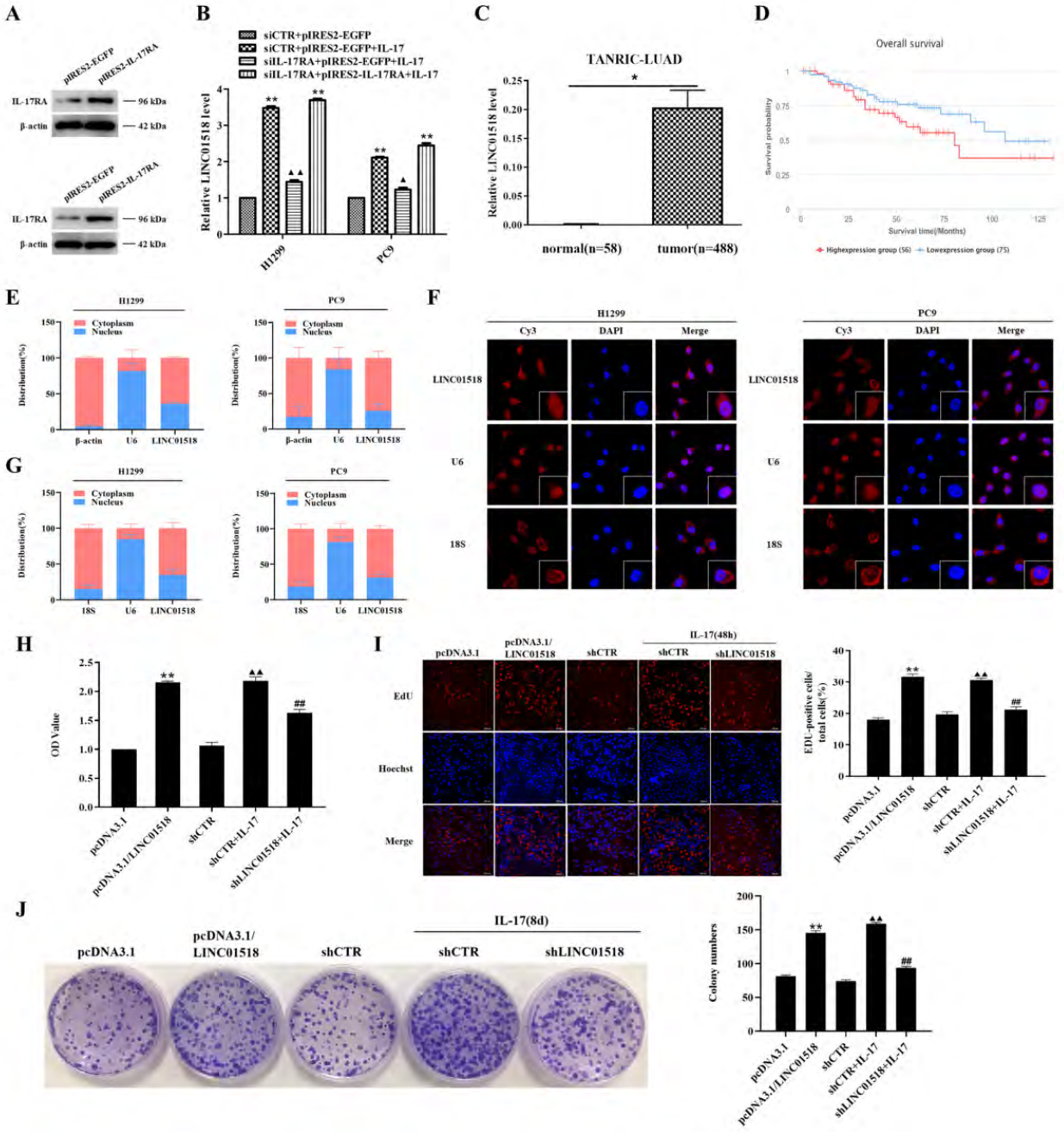

Fig. 3 [Download full resolution image]

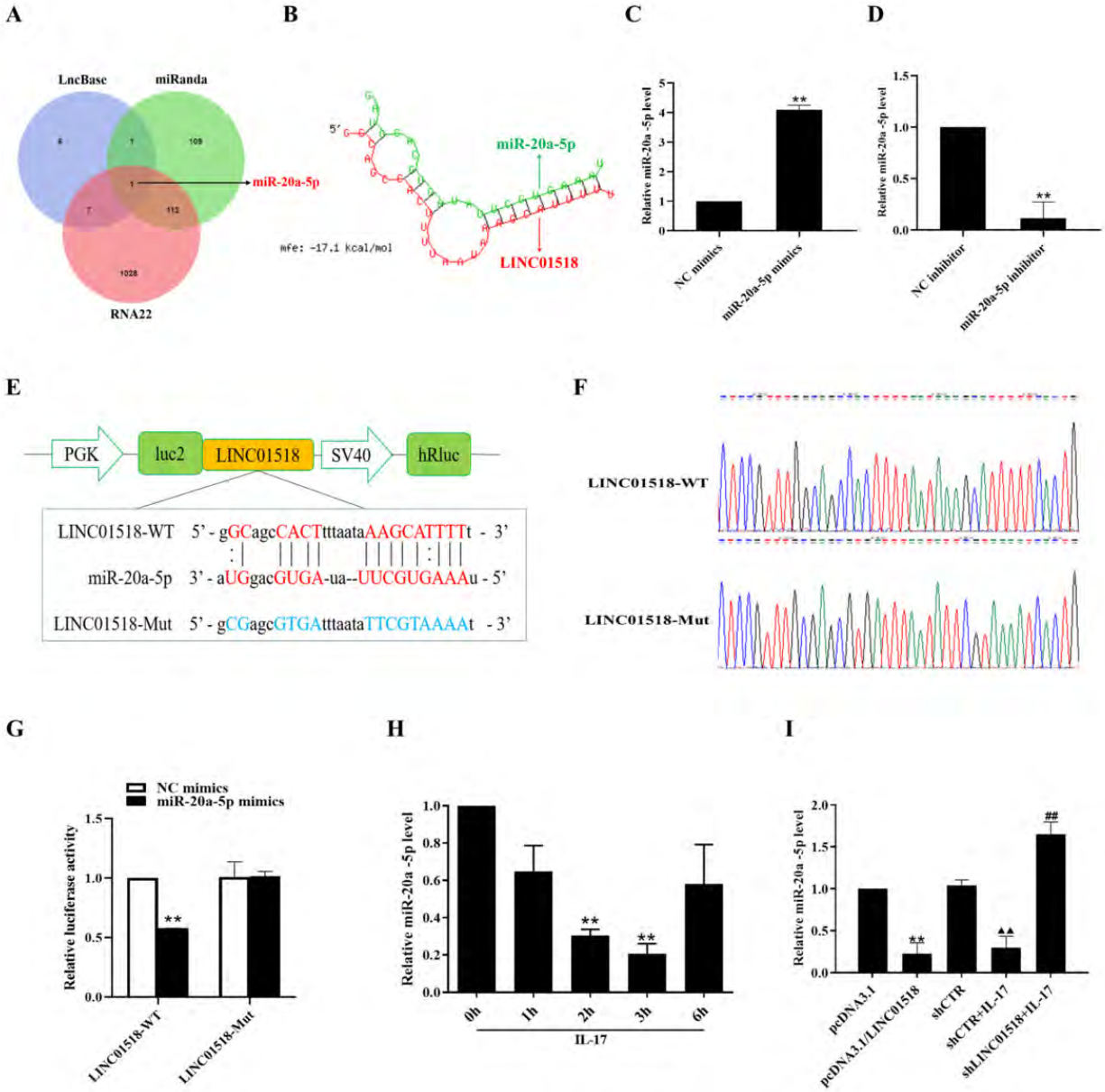

Fig. 4 [Download full resolution image]

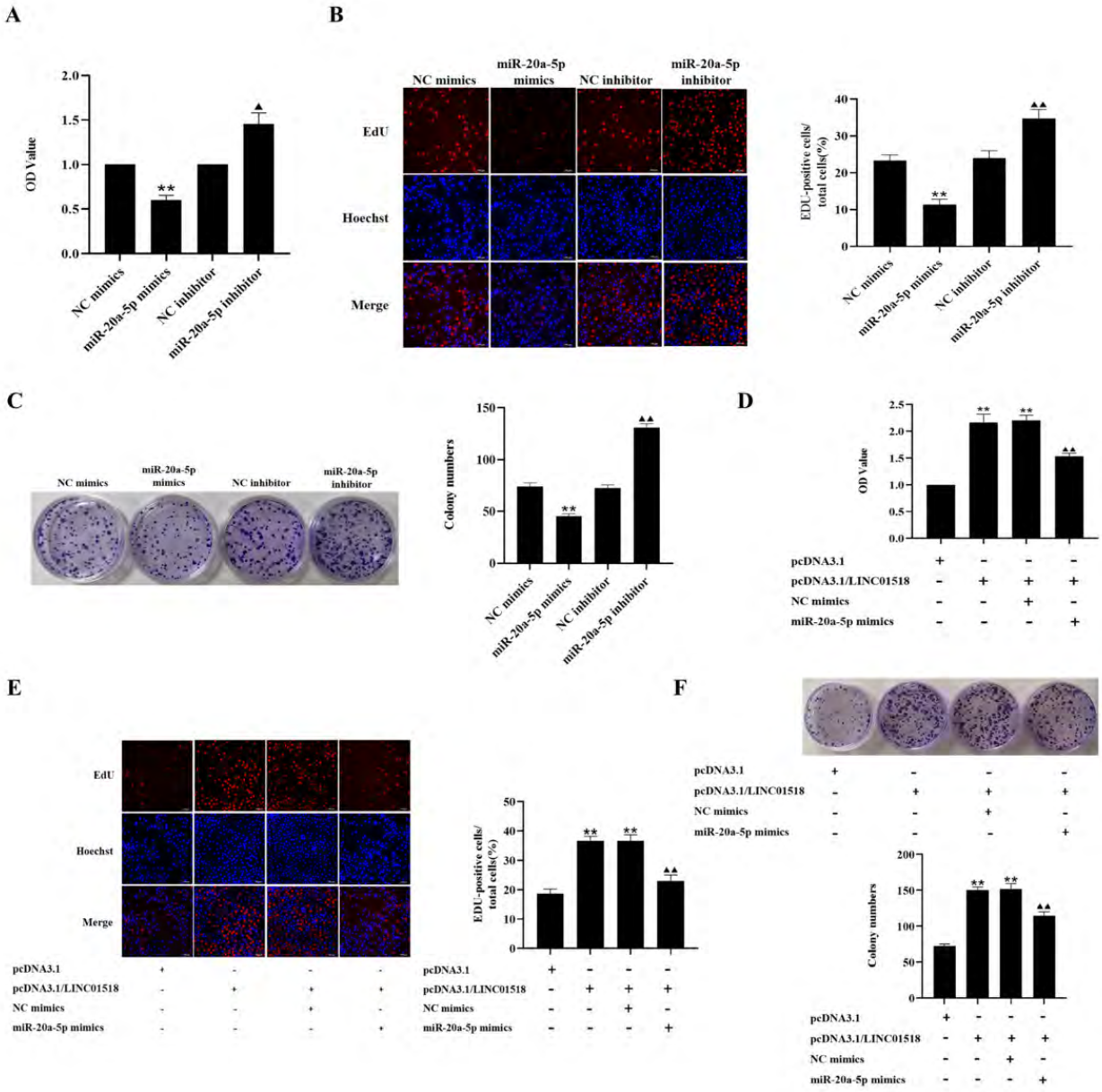

Fig. 5 [Download full resolution image]

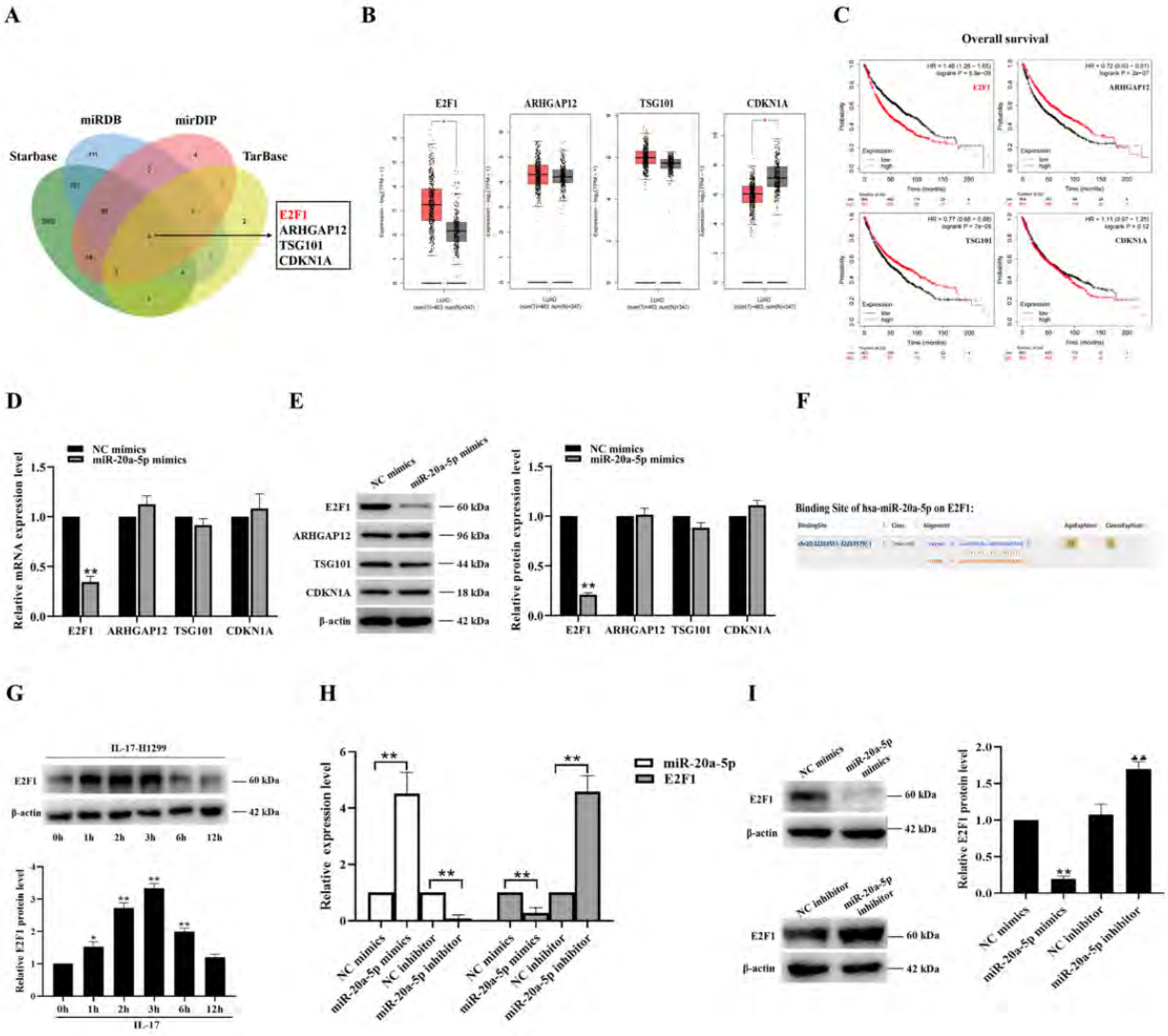

Fig. 6 [Download full resolution image]

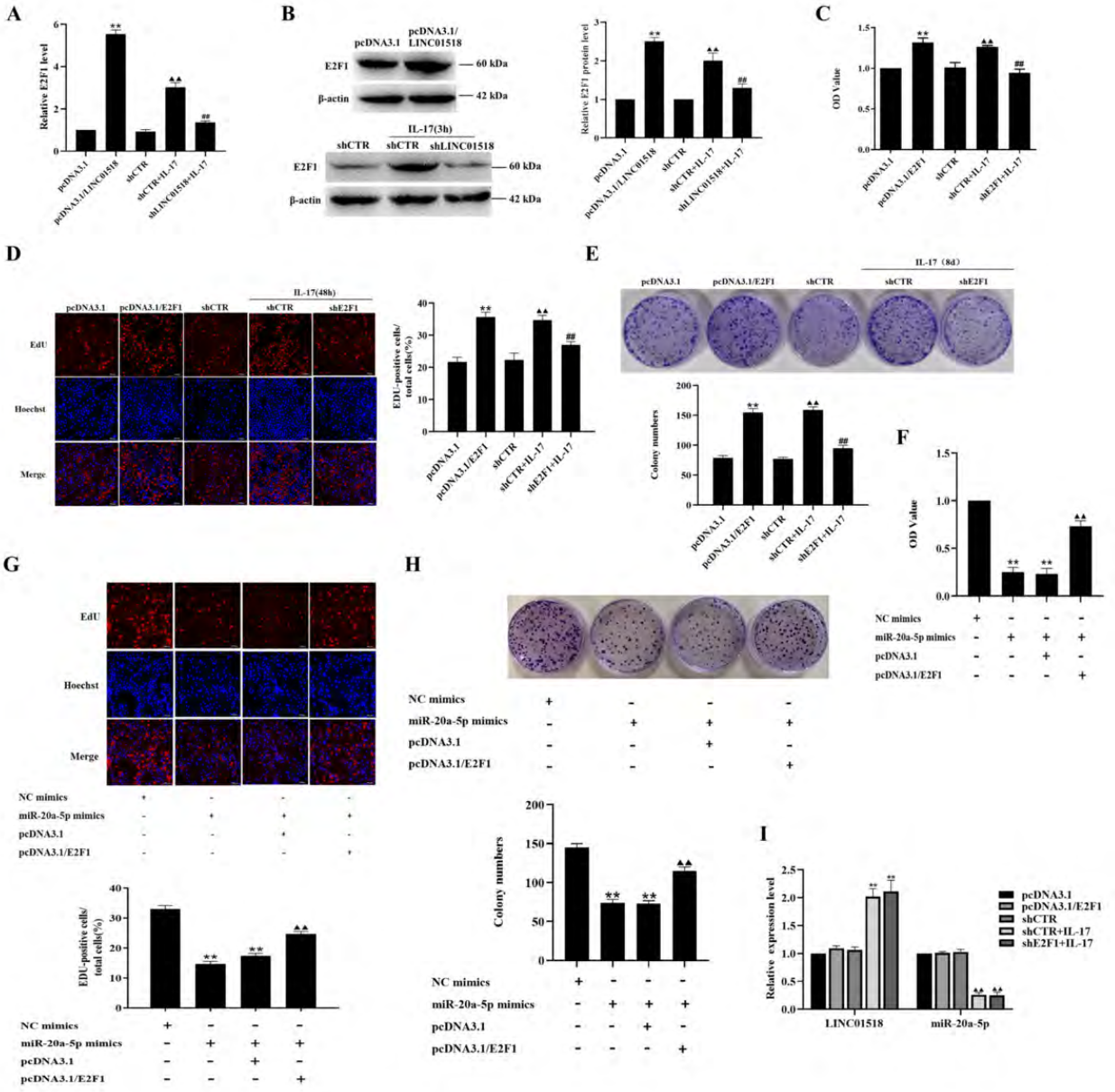

Fig. 7 Download full resolution image